

Active Steer Control System of Front and Rear Wheels through Reference Model Following Control Based on Driver's Sense Characteristics

journal or publication title	Bulletin of Kurume Institute of Technology
number	34
page range	11-28
year	2012-03-20
URL	http://id.nii.ac.jp/1503/00000058/

〔論文〕

Active Steer Control System of Front and Rear Wheels through Reference Model Following Control Based on Driver's Sense Characteristics

Kazunori MORI

Abstract

We specify a new control method based on driver's sense characteristics for active steer control system of front and rear wheels. Vehicles equipped with this four-wheel-active steering system can independently control two state variables of yaw rate, and lateral acceleration or body slip angle because the system has two control inputs of the front and rear wheel steer angles. In other words, the yawing motion of the vehicle, and the lateral motion or the direction of the body to the traveling direction in the vehicle can be controlled simultaneously and independently. Then, paying attention to yaw rate characteristics and yaw center location, we have proposed a method of setting concrete control objectives to achieve vehicle characteristics that drive easily through the four-wheel active-steer control. Next, we obtained the control rule of this system that combines the steering angle feed forward control with the vehicle state variables feedback control to achieve the target characteristics of yaw rate to have form of 1st/2nd order and to adjust the yaw center to a prescribed position. Computer simulation confirmed that when the vehicle applied this steering control system, the effects of control for improving the vehicle performance were great.

Keywords : Vehicle Dynamics, Maneuverability, Stability, Motion Control, Active Steer Control, Four-Wheel-Steering, Front and Rear Wheels-Active Steering System, Driver-Vehicle System, Sense Characteristic

1 . Introduction

In order to improve automobile performance, various research has been done regarding the vehicle motion characteristics of yaw rate, body slip angle, lateral acceleration etc. to the operating angle of the steering wheel. The results of these studies have been used for automotive development. Such the fundamental research as the driver-vehicle system has been applied to the vehicle dynamics control field, and the results of various research and development have been contributing to improve the active safety of automobiles.

When the control rules of four-wheel-steering and distribution control device of driving/braking forces of the vehicle are derived, various methods have been proposed: setting the body slip angle at the center of gravity to zero⁽¹⁾, locating the yaw center to an appropriate positions⁽²⁾, setting the transfer function on yaw rate characteristic to steering wheel angle to the first delay element⁽³⁾ or to the 1st/2nd form element, etc., as a target performance (reference model). Recently, many vehicle control devices through these proposed control laws have been put to practical use.

*交通機械工学科
平成23年9月6日受理

Four-wheel active-steer control system (active steer control system of front and rear wheels) can independently control two among vehicle motion state variables of yaw rate, lateral acceleration, and body slip angle because it has two control inputs of the front and rear wheel steer angles. In a word, this system can control the yawing motion of the vehicle, and the lateral motion or the direction of the body to the traveling direction in the vehicle simultaneously and independently. Setting both the gains of frequency response of yaw rate and lateral acceleration to be constant⁽⁴⁾, both the transfer functions on yaw rate and lateral acceleration to steering wheel angle to the first delay characteristics⁽⁵⁾, cooperative control of setting the yaw rate characteristic to the first delay element and of making the yaw center an arbitrary position⁽⁶⁾, and both the transfer functions on yaw rate and body slip angle at the center of gravity to the first delay characteristics through the cooperative control with the wheel steer control and the distribution control of braking forces⁽⁷⁾, etc. have been proposed for the control rule of active steering system as the target performances. Recently, a four-wheel active-steer control system of the steering angle feed forward control method to set both the transfer functions on yaw rate and body slip angle to the 1st/second form characteristics was put to practical use⁽⁸⁾. However, neither each coefficient value of the target characteristic of this device nor the decision process of the control rule etc. has been made public.

Analyzing the vehicle motion of 2WS (two-wheel-steering:average vehicle with front wheel steering) by using two-wheel model for maneuverability and stability analysis, the transfer functions on yaw rate and body slip angle to steering wheel angle are both the first/second form elements. Moreover, at the early stage of automotive development, such the vehicle steer characteristics as understeer cornering characteristic, steady gain, yaw rate resonance frequency, phase lag angle at steering frequency 1 [Hz], and ratio of static/dynamic gain on the yaw rate frequency response to steering wheel angle, and lateral acceleration characteristics etc. are often used as the general target performance values of vehicle dynamics capability. Making the yaw rate characteristic the first/second form element when we set up the target control performance, we are able to compare the target characteristic and the performance difference with the characteristic of 2WS easily.

In this paper, we propose the method of setting the concrete control objective to make the vehicle motion characteristics to drive easily by the active steer control system of front and rear wheels that pays attention to the yaw rate characteristic and the yaw center location. Next, we derive a control rule of the four-wheel active-steer control system that combines the feed forward control of steering wheel angle and the feedback control of vehicle state variables, which sets the yaw rate characteristic to a target transfer function of the first/second form and makes the yaw center a prescribed position. In Addition, computer simulation clarifies the control effects of this system.

2 . Nomenclature

The notations used in vehicle model for theoretical analysis and the main parameters and characteristic values used to calculate are listed below.

F_r : sum of two cornering forces of right and left tires

I_z : yaw moment of inertia {2400kgm²}

K : stability factor

K_r : equivalent cornering power {33.7, 50.5 kN/rad}

N : steering overall gear ratio {15.4}

a, b : distance from front/rear axle to center of gravity of vehicle {1.18, 1.44m}

e : distance from yaw center to center of gravity of vehicle---The rear side of the vehicle is defined from center of gravity as +.

l : wheelbase {2.62m}
 m : vehicle mass {1500kg}
 r : yaw rate
 s, t : Laplace transform operator, time
 V : vehicle velocity
 α_y : lateral acceleration of vehicle
 α_i : tire sideslip angle
 β : body sideslip angle at c.g. of vehicle
 δ_i : front/rear wheel steer angle
 θ : steering wheel angle
 Subscript
 i : f-front wheels, r-rear wheels
 Coordinates
 o - xy , O - XY : coordinates fixed to the vehicle body, coordinates fixed to the road

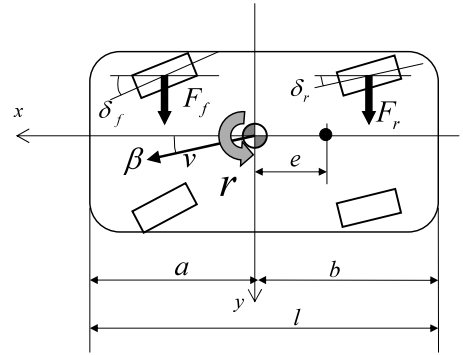


Fig.1 Theoretical analysis model

3 . Target characteristics of vehicle

3.1 Equations of vehicle motion

The calculating model for the analysis of vehicle dynamics is illustrated in Figure 1. When the cornering characteristics of right and left tires are assumed to be the same, the vehicle motion equations are as follows. The explanations of the notation used in the equations etc. are listed in the appendix in the tail of this paper.

$$mV(\dot{\beta} + r) = F_f + F_r \quad \dots \dots \dots (1)$$

$$I_z \dot{r} = aF_f - bF_r \quad \dots \dots \dots (2)$$

Each cornering force generated in the front and rear tires is given by the following equation.

$$F_f = 2K_f \alpha_f \quad \dots \dots \dots (3)$$

$$F_r = 2K_r \alpha_r \quad \dots \dots \dots (3)$$

Equation (4) yields the sideslip angle of each tire in Eq. (3).

$$\left. \begin{aligned} \alpha_f &= \delta_f - \beta - \frac{a}{V} r \\ \alpha_r &= \delta_r - \beta + \frac{b}{V} r \end{aligned} \right\} \quad \dots \dots \dots (4)$$

Equations (1) ~ (4) are combined in the form of a matrix equation on the body sideslip angle β and the yaw rate r , and the following equation is obtained.

$$\begin{bmatrix} \dot{\beta} \\ \dot{r} \end{bmatrix} = \begin{bmatrix} p_{11}(s) & p_{12}(s) \\ p_{21}(s) & p_{22}(s) \end{bmatrix} \begin{bmatrix} \delta_f \\ \delta_r \end{bmatrix} = P \begin{bmatrix} \delta_f \\ \delta_r \end{bmatrix} \quad \dots \dots \dots (5)$$

where

$$\left. \begin{aligned} P_{11}(s) &= \frac{G_{\beta 1} \omega_n^2 (\tau_{\beta 1} s + 1)}{s^2 + 2\zeta \omega_n s + \omega_n^2} \\ P_{12}(s) &= \frac{G_{\beta 2} \omega_n^2 (\tau_{\beta 2} s + 1)}{s^2 + 2\zeta \omega_n s + \omega_n^2} \\ P_{21}(s) &= \frac{G_{r 1} \omega_n^2 (\tau_{r 1} s + 1)}{s^2 + 2\zeta \omega_n s + \omega_n^2} \\ P_{22}(s) &= \frac{G_{r 2} \omega_n^2 (\tau_{r 2} s + 1)}{s^2 + 2\zeta \omega_n s + \omega_n^2} \end{aligned} \right\} \quad \dots \dots \dots (6)$$

Details of each coefficient at the right of Eq. (6) are listed in the appendix. Here, ω_n and ζ show the natural angular frequency and the damping coefficient ratio respectively. Moreover, this product $\zeta\omega_n$ is called the dumping coefficient.

Because the relations of $\delta_f = \theta/N$, $\delta_r = 0$ consist in 2 WS, two relations of $\beta = p_{11}(s)\theta/N$, $r = p_{21}(s)\theta/N$ are given by Eq. (5). Both transfer functions of yaw rate and body slip angle at center of gravity to steering wheel angle are shown in the form of first/second for Laplace transform operator s .

3.2 Yaw rate characteristics

When various factors closely related to driver's sense characteristics are calculated about yaw rate characteristics of 2WS, the following equations are obtained.

① Steady gain:

Using the third equation of Eq. (6), the steady gain on yaw rate frequency response is $p_{21}(0)/N$. Moreover, the steady gain is given by the next equation.

$$\left(\frac{r}{\theta}\right)_0 = \frac{G_{r1}}{N} = \frac{V}{NI(1 + KV^2)} \quad \dots \dots \dots (7)$$

② Yaw rate resonance frequency:

Angular frequency ω that makes gain $|p_{21}(j\omega)|$ the maximum yields a yaw rate resonance frequency. When this angular frequency ω is described by ω_p [rad/s], the next equation gives the yaw rate resonance frequency f_p [Hz].

$$f_p = \frac{\omega_p}{2\pi} = \frac{\sqrt{-1 + \sqrt{1 + \tau_{r1}^2 \omega_n^2 (2 - 4\zeta^2 + \tau_{r1}^2 \omega_n^2)}}}{2\pi\tau_{r1}} \quad \dots \dots \dots (8)$$

$$\text{where } |\zeta| \leq \frac{\sqrt{2 + \tau_{r1}^2 \omega_n^2}}{2}$$

③ Ratio of static/dynamic gain on the yaw rate frequency response:

Described by $\hat{r} = r(j\omega)/\delta_f(j\omega) = p_{21}(j\omega)$, gain $|\hat{r}|$ and phase angle $\angle \hat{r}$ are given respectively by the next equations.

$$|\hat{r}| = G_{r1} \omega_n^2 \sqrt{\frac{1 + \omega^2 \tau_{r1}^2}{(\omega_n^2 - \omega^2)^2 + (2\zeta\omega_n\omega)^2}} \quad \dots \dots \dots (9)$$

$$\angle \hat{r} = \tan^{-1} \frac{\omega \{ \tau_{r1} (\omega_n^2 - \omega^2) - 2\zeta\omega_n \}}{(2\zeta\omega_n\tau_{r1} - 1)\omega^2 + \omega_n^2} \quad \dots \dots \dots (10)$$

When the gain at $\omega = \omega_p$ is described by G_p , that is given by the next equation.

$$G_p = |\hat{r}|_p = G_{r1} \sqrt{\frac{1 + \omega_p^2 \tau_{r1}^2}{\{1 - (\omega_p/\omega_n)^2\}^2 + 4\zeta^2 (\omega_p/\omega_n)^2}} \quad \dots \dots \dots (11)$$

Therefore, G_p/G_{r1} yields the ratio of static/dynamic gain on the yaw rate frequency response to steering wheel angle.

④ Phase delay at 1 [Hz]:

When the phase lag degree at 1 [Hz] on yaw rate frequency response described by, $\angle \hat{r}_1$ that is given by the next equation.

$$\angle \hat{r}_1 = \tan^{-1} \frac{\omega_1 \{ \tau_{r1} (\omega_n^2 - \omega_1^2) - 2\zeta\omega_n \}}{(2\zeta\omega_n\tau_{r1} - 1)\omega_1^2 + \omega_n^2} \quad \dots \dots \dots (12)$$

3.3 Vehicle motion characteristics that drive easily

Regarding to the vehicle motion characteristics that drive easily, the findings that have been used on actual vehicle development sites over many years and numerous research reports exist. In this section, we address many of the findings that resolve compound phenomenon in closed loop of driver-vehicle system to each element, and replace it with quantitative target value of open loop characteristic of vehicle⁽⁹⁾, and the contents known well in the research of vehicle dynamics control etc. , as examples.

The cornering characteristic of vehicle is a main factor, and this can be shown by a stability factor K . In general, K is set to about $1.0 \times 10^{-3} \sim 3.5 \times 10^{-3} [\text{s}^2/\text{m}^2]$. For instance, a sporty automobile reduces K to weaken understeer characteristic, K is usually set on the difference by the vehicle concept. Moreover, by conducting a mock driving experiment using a driving simulator⁽¹⁰⁾, we have obtained the result that the driver tends to like the vehicle with a weak understeer characteristic which improves driving proficiency.

The target characteristic values of the yaw rate frequency response to steering wheel angle include the steady gain, resonance frequency, phase delay, and damping coefficient etc.. Steady gain of Eq. (7) relates closely to the stability factor that quantitatively shows the vehicle cornering characteristic. The steady gain is often used when comparing it as a target characteristic of the steer control system with 2WS, and it is enlarged in the range from low velocity to the medium velocity to achieve the movement of an energetic vehicle to the steering wheel operating, and slightly reduced in the high velocity range to secure stability.

Next, making the vehicle motion follow also to a quick steering wheel operation, the yaw rate natural frequency $f_n = \omega_n / 2\pi$ in Eq. (6) and the yaw rate resonance frequency f_p of Eq. (8) are raised as much as possible. With this, the phase lag (which assumes representative value at 1 [Hz]) usually decreases as well. The damping coefficient $S\omega_n$, that is the product of the damping coefficient ratio S and the natural angular frequency ω_n , in Eq. (6) is enlarged as much as possible, and the damping characteristics are improved⁽¹¹⁾. In general, if the cornering power of the front and rear tires is raised, the damping coefficient grows. Moreover, there is the ratio of static/dynamic gain G_p/G_r in Eq. (11) as one of the damping characteristic indices, and it has been reported that adjusting this ratio to about 12 improves driving control the most⁽¹²⁾.

In the frequency response of lateral acceleration to steering wheel operation, because steady lateral acceleration is a product of steady yaw rate and vehicle velocity, it is important to think about the balance of steady gains of lateral acceleration and yaw rate in the static response. And, it is necessary for the improvement of dynamic response to reduce the decrease of the gain and of the phase delay in the range of 1 [Hz] or more on the steering wheel operating frequency. Especially, there has been a report of obtaining an excellent control result when the difference of phase lag between yaw rate and lateral acceleration is reduced⁽¹³⁾.

The idea that it is easy to drive arose from the research of the four-wheel steering if the body slip angle at c.g. of the vehicle is adjusted to zero, in a word the direction of the body is matched to the traveling direction. And, the four-wheel steering to which this idea was taken was put to practical use⁽¹⁴⁾. Because the position in which the driver sits and the c.g. of the vehicle body are almost the same, this idea is approved for a general passenger car. However, an automobile such as a 1box type is greatly different from these positions.

Then, there is a yaw center in the one that this idea was enhanced^(15,16). The yaw center is a instantaneous center of vehicle in the cornering movement. If this position is corresponding to the c.g. of the vehicle, it means that the body slip angle is the same as zero. Theoretically, the more it moves the yaw center behind the vehicle, the more the understeer strengthens.

As mentioned above, there are a lot of findings also in the open loop characteristic of the vehicle that drives easily, and each evaluation figure is related combining.

In this report, we take up the reference model following control to set the target transfer function of yaw

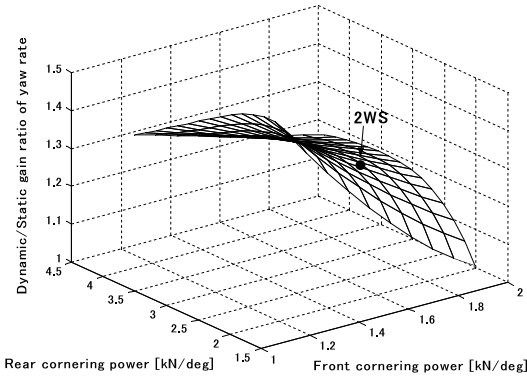


Fig.2 Relationship between cornering power and yaw rate dynamic/static gain ratio

rate to have form of the first/second order and to achieve the target characteristic of body sideslip angle at the same time or to adjust the yaw center to a prescribed position, as a typical example energizing the feature of the four-wheel active-steer control that can independently control lateral and rotary motions of a vehicle.

3.4 Setting of target characteristics

The comparison of the performances is easy because it is in the form of the same first/second as the case of 2WS without the control when the yaw rate characteristic of the target sets up to the first/second form.

We assume the cornering powers of the front wheel and the rear wheel to be two parameters, calculate the target characteristics described in clause 3.3, and graph. The calculation uses the parameters and the characteristic values of a compact passenger car class in the appendix. Figure 2 shows the changing of static/dynamic gain ratio on yaw rate frequency response to the front and rear cornering powers. They changed the value of each 85.5 [N/deg] and 171.0 [N/deg] respectively. The black circle sign indicates the values of the cornering power of 2WS and the ratio of static/dynamic gain.

Figure 3 shows the relationship between yaw rate resonance frequency and yaw rate damping. Figure 4 shows the relationship between yaw rate resonance frequency and stability factor. As one example, the white circle sign is a command of the target characteristic using to the calculation in the future. The objective characteristics set the stability factor to the same as 2WS, the yaw damping coefficient to 8.04 [1/s], and the yaw rate resonance frequency to 1.52 [Hz]. The target value of τ_n in Eq. (6) set up to the same as 2WS though it doesn't show in figures. In addition, these commands yield the natural frequency of yaw rate, the static/dynamic gain ratio on yaw rate, and the phase lag angle of yaw rate at 1Hz, those are given respectively by 1.60 [Hz], 1.18, and -14.3 [deg].

Though the target vehicle dynamics performances are simply a collection of the vehicle characteristics

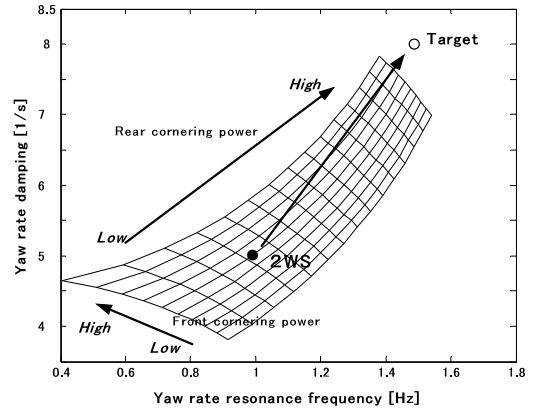


Fig.3 Relationship between yaw rate resonance frequency and yaw rate damping

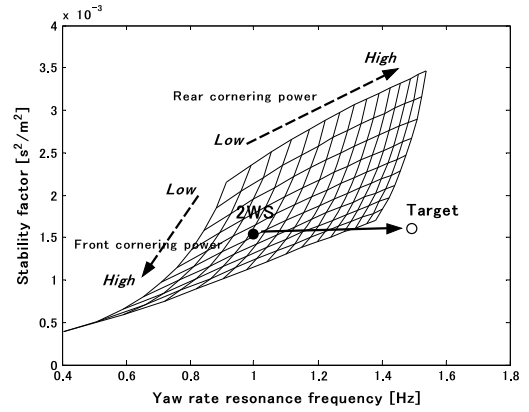


Fig.4 Relationship between yaw rate resonance frequency and stability factor

that drive easily in clause 3.3, we can understand that it is impossible to achieve them with 2 WS from Figures 2 ~ 4. Then, we show that active-steering control can achieve those target characteristics below the following clause. In addition, because the active steer control system of front and rear wheels can control to fix a yaw center to an arbitrary position, we can add $e=0$ to the target characteristic.

4 . Control method of four-wheel active-steering

4.1 Expression in the form of state equation

Transforming Eqs. (1) ~ (4) of the vehicle motion equations into the form of a state equation, we obtain Eq. (13).

$$\left. \begin{array}{l} \dot{\mathbf{x}} = \mathbf{Ax} + \mathbf{Bu} \\ \mathbf{y} = \mathbf{Cx} = \mathbf{x} \end{array} \right\} \dots \dots \dots (13)$$

where

$$\mathbf{x} = [\beta \ r]^T, \ \mathbf{u} = [\delta_f \ \delta_r]^T$$

And, $\mathbf{y}=\mathbf{x}$, each coefficient matrix is as follows.

$$\mathbf{A} = \begin{bmatrix} -\frac{2(K_f + K_r)}{mV} & -\frac{mV^2 + 2(bK_r - aK_f)}{mV^2} \\ \frac{2(bK_r - aK_f)}{I_z} & -\frac{2(a^2K_f + b^2K_r)}{I_zV} \end{bmatrix}$$

$$\mathbf{B} = \begin{bmatrix} \frac{2K_f}{mV} & \frac{2K_r}{mV} \\ \frac{2aK_r}{I_z} & -\frac{2bK_r}{I_z} \end{bmatrix}, \ \mathbf{C} = \mathbf{I}_{2 \times 2} = \begin{bmatrix} 1 & 0 \\ 0 & 1 \end{bmatrix}$$

4.2 Reference model

We consider three cases in which yaw rate and body sideslip angle, or yaw center position are assumed to be objective performances. And, the expression by a concrete equation of the target characteristic is defined as the reference model.

① In the case of setting two target transfer functions of body sideslip angle and yaw rate to steering wheel angle to both the first/second order form for s respectively:

When objective body sideslip angle and yaw rate are described respectively by β_m and r_m , two reference models are given by the next transfer functions.

$$\frac{\beta_m(s)}{\theta(s)} = \frac{\bar{b}_1s + \bar{b}_0}{s^2 + \bar{a}_{11}s + \bar{a}_{10}} \dots \dots \dots (14)$$

$$\frac{r_m(s)}{\theta(s)} = \frac{\bar{c}_1s + \bar{c}_0}{s^2 + \bar{a}_{21}s + \bar{a}_{20}} \dots \dots \dots (15)$$

where

$$\bar{a}_{11} = 2\bar{\zeta}_\beta \bar{\omega}_{n\beta}, \ \bar{a}_{10} = \bar{\omega}_{n\beta}^2, \ \bar{b}_1 = G_{m\beta 1} \bar{c}_\beta \bar{\omega}_{n\beta}^2, \ \bar{b}_0 = G_{m\beta 1} \bar{\omega}_{n\beta}^2$$

$$\bar{a}_{21} = 2\bar{\zeta}_r \bar{\omega}_{nr}, \ \bar{a}_{20} = \bar{\omega}_{nr}^2, \ \bar{c}_1 = G_{mr 1} \bar{c}_r \bar{\omega}_{nr}^2, \ \bar{c}_0 = G_{mr 1} \bar{\omega}_{nr}^2$$

Here, when the equivalent steering gear ratio N_e is defined, $G_{m\beta 1} = G_{\beta 1}/N_e$, $G_{mr 1} = G_{r 1}/N_e$ are obtained.

Equation (14) is divided into two of the next equations.

$$\left. \begin{aligned} \frac{x_m(s)}{\theta(s)} &= \frac{1}{s^2 + \bar{a}_{11}s + \bar{a}_{10}} \\ \frac{\beta_m(s)}{x_m} &= \bar{b}_1s + \bar{b}_0 \end{aligned} \right\} \dots \dots \dots (16)$$

Because there is a relation of $(s^2 + \bar{a}_{11}s + \bar{a}_{10})x_m(s) = \theta(s)$ in the first equation of Eq. (16), $\ddot{x}_m + \bar{a}_{11}\dot{x}_m + \bar{a}_{10}x_m = \theta$ is obtained by using inverse Laplace transform.

When $x_{m1} = x_m$, $x_{m2} = \dot{x}_{m1}$ are defined, $\dot{x}_{m1} = \dot{x}_m = x_{m2}$, $\dot{x}_{m2} = \ddot{x}_{m1} = \ddot{x}_m$ are obtained.

And next equations are derived.

$$\begin{aligned} \dot{x}_{m1} &= -\bar{a}_{10}x_{m1} - \bar{a}_{11}\dot{x}_{m1} + \theta \\ \dot{x}_{m2} &= -\bar{a}_{10}x_{m1} - \bar{a}_{11}\dot{x}_{m2} + \theta \end{aligned}$$

Therefore, these equations are brought together in the next state equation.

$$\begin{bmatrix} \dot{x}_{m1} \\ \dot{x}_{m2} \end{bmatrix} = \begin{bmatrix} 0 & 1 \\ -\bar{a}_{10} & -\bar{a}_{11} \end{bmatrix} \begin{bmatrix} x_{m1} \\ x_{m2} \end{bmatrix} + \begin{bmatrix} 0 \\ 1 \end{bmatrix} \theta \dots \dots \dots (17)$$

Moreover, because there is a relation of $\beta_m(s) = (\bar{b}_1s + \bar{b}_0)x_m(s)$ in the second equation of Eq. (16), $\beta_m = \bar{b}_1\dot{x}_m + \bar{b}_0x_m = \bar{b}_1x_{m2} + \bar{b}_0x_{m1}$ is obtained by using inverse Laplace transform. This equation is transformed to the next state equation.

$$\beta_m = [\bar{b}_0 \ \bar{b}_1] \begin{bmatrix} x_{m1} \\ x_{m2} \end{bmatrix} \dots \dots \dots (18)$$

Bringing together Eq. (17) and Eq. (18) in one equation, the next state equation is obtained.

$$\left. \begin{aligned} \dot{\mathbf{x}}_{m\beta} &= \mathbf{A}_{m\beta}\mathbf{x}_{m\beta} + \mathbf{b}_{m\beta}\theta \\ y_{m\beta} &= \mathbf{c}_{m\beta}^T\mathbf{x}_{m\beta} \end{aligned} \right\} \dots \dots \dots (19)$$

where

$$\mathbf{x}_{m\beta} = \begin{bmatrix} x_{m1} \\ x_{m2} \end{bmatrix}, \mathbf{A}_{m\beta} = \begin{bmatrix} 0 & 1 \\ -\bar{a}_{10} & -\bar{a}_{11} \end{bmatrix}, \mathbf{b}_{m\beta} = \begin{bmatrix} 0 \\ 1 \end{bmatrix}, y_{m\beta} = \beta_m, \mathbf{c}_{m\beta} = \begin{bmatrix} \bar{b}_0 \\ \bar{b}_1 \end{bmatrix}$$

In addition, similarly transforming for the target characteristic of yaw rate, and bringing it together in one equation with Eq. (19), the next state equation is obtained.

$$\left. \begin{aligned} \dot{\mathbf{x}}_m &= \mathbf{A}_m\mathbf{x}_m + \mathbf{b}_m\theta \\ y_m &= \mathbf{C}_m\mathbf{x}_m \end{aligned} \right\} \dots \dots \dots (20)$$

where

$$\begin{aligned} \mathbf{x}_m = \begin{bmatrix} \mathbf{x}_{m\beta} \\ \mathbf{x}_{mr} \end{bmatrix} &= \begin{bmatrix} x_{m1} \\ x_{m2} \\ x_{m3} \\ x_{m4} \end{bmatrix}, \mathbf{A}_m = \begin{bmatrix} 0 & 1 & 0 & 0 \\ -\bar{a}_{10} & -\bar{a}_{11} & 0 & 0 \\ 0 & 0 & 0 & 1 \\ 0 & 0 & -\bar{a}_{20} & -\bar{a}_{21} \end{bmatrix}, \mathbf{b}_m = \begin{bmatrix} \mathbf{b}_{m\beta} \\ \mathbf{b}_{mr} \end{bmatrix} = [0 \ 1 \ 0 \ 1]^T \\ y_m = \begin{bmatrix} y_{m\beta} \\ y_{mr} \end{bmatrix} &= \begin{bmatrix} \beta_m \\ r_m \end{bmatrix}, \mathbf{C}_m = \begin{bmatrix} \bar{b}_0 & \bar{b}_1 & 0 & 0 \\ 0 & 0 & \bar{c}_0 & \bar{c}_1 \end{bmatrix} \end{aligned}$$

② In the case of setting the target transfer function of body sideslip angle to steering wheel angle to the first delay element, and one of yaw rate to the first/second order form:

The reference models are shown by the following two transfer functions.

$$\frac{\beta_m(s)}{\theta(s)} = \frac{G_{m\beta 1}}{1 + \tau_\beta s} \dots \dots \dots (21)$$

$$\frac{r_m(s)}{\theta(s)} = \frac{\bar{c}_1s + \bar{c}_0}{s^2 + \bar{a}_{21}s + \bar{a}_{20}} \dots \dots \dots (15)'$$

Transforming Eq. (21) yields the next equation.

$$\dot{\beta}_m = -\frac{1}{\tau_\beta} \beta_m + \frac{G_{m\beta 1}}{\tau_\beta} \theta \quad \dots \dots \dots (22)$$

When $\beta_m = x_{m\beta} = x_{m1}$, $y_{m\beta} = \beta_m = x_{m1}$ are defined, Eq. (22) is rewritten as follows.

$$\dot{x}_{m1} = -\frac{1}{\tau_\beta} x_{m1} + \frac{G_{m\beta 1}}{\tau_\beta} \theta \quad \dots \dots \dots (23)$$

Equation (15)' is transformed as follows in the case to lead Eqs. (17) ~ (19) in a similar way.

When, $x_{m3} = x_m$, $x_{m4} = \dot{x}_{m3}$ are defined, the following equations are derived.

$$\dot{\mathbf{x}}_{mr} = \begin{bmatrix} \dot{x}_{m3} \\ \dot{x}_{m4} \end{bmatrix} = \begin{bmatrix} 0 & 1 \\ -\bar{a}_{20} & -\bar{a}_{21} \end{bmatrix} \begin{bmatrix} x_{m3} \\ x_{m4} \end{bmatrix} + \begin{bmatrix} 0 \\ 1 \end{bmatrix} \theta \quad \dots \dots \dots (24)$$

$$y_{mr} = r_m = \begin{bmatrix} \bar{c}_0 & \bar{c}_1 \end{bmatrix} \begin{bmatrix} x_{m3} \\ x_{m4} \end{bmatrix} \quad \dots \dots \dots (25)$$

$$\left. \begin{aligned} \dot{\mathbf{x}}_{mr} &= \mathbf{A}_{mr} \mathbf{x}_{mr} + \mathbf{b}_{mr} \theta \\ y_{mr} &= \mathbf{C}_{mr}^T \mathbf{x}_{mr} \end{aligned} \right\} \quad \dots \dots \dots (26)$$

Bringing together Eq. (23) and Eq. (26) yields the next state equation.

$$\left. \begin{aligned} \dot{\mathbf{x}}_m &= \mathbf{A}_m \mathbf{x}_m + \mathbf{b}_m \theta \\ \mathbf{y}_m &= \mathbf{C}_m \mathbf{x}_m \end{aligned} \right\} \quad \dots \dots \dots (27)$$

where

$$\mathbf{x}_m = \begin{bmatrix} x_{m\beta} \\ \mathbf{x}_{mr} \end{bmatrix} = \begin{bmatrix} x_{m1} \\ x_{m3} \\ x_{m4} \end{bmatrix}, \mathbf{A}_m = \begin{bmatrix} -1/\tau_\beta & 0 & 0 \\ 0 & 0 & 1 \\ 0 & -\bar{a}_{20} & -\bar{a}_{21} \end{bmatrix}$$

$$\mathbf{b}_m = \begin{bmatrix} b_{m\beta} \\ \mathbf{b}_{mr} \end{bmatrix} = \begin{bmatrix} G_{m\beta 1}/\tau_\beta & 0 & 1 \end{bmatrix}^T$$

$$\mathbf{y}_m = \begin{bmatrix} y_{m\beta} \\ y_{mr} \end{bmatrix} = \begin{bmatrix} \beta_m \\ r_m \end{bmatrix}, \mathbf{C}_m = \begin{bmatrix} 1 & 0 & 0 \\ 0 & \bar{c}_0 & \bar{c}_1 \end{bmatrix}$$

③ In the case of setting the target transfer function of yaw rate to steering wheel angle to the first/second form and of making the yaw center a prescribed position.

When a yaw center is at the position of the distance of e from the body center of gravity to the rear side, the moving velocity to horizontal direction \dot{y}_e is zero at this point. Therefore, $\dot{y}_e = \dot{y} - er = 0$ is obtained.

$\beta = er/V$ is led from $\beta = \dot{y}/V$. Therefore, we can understand that body sideslip angle and yaw rate are related each other. When a prescribed yaw center position is e_m , the reference models are shown by the following two equations.

$$\beta_m = \frac{e_m r_m}{V} \quad \dots \dots \dots (28)$$

$$\frac{r_m(s)}{\theta(s)} = \frac{\bar{c}_1 s + \bar{c}_0}{s^2 + \bar{a}_{21} s + \bar{a}_{20}} \quad \dots \dots \dots (15)''$$

The following equation is obtained from Eq. (28).

$$\frac{\beta_m(s)}{\theta(s)} = \frac{e_m}{V} \cdot \frac{r_m}{\theta} = \frac{e_m}{V} \cdot \frac{\bar{c}_1 s + \bar{c}_0}{s^2 + \bar{a}_{21} s + \bar{a}_{20}} = \frac{\bar{b}_1 s + \bar{b}_0}{s^2 + \bar{a}_{11} s + \bar{a}_{10}} \quad \dots \dots \dots (29)$$

where

$$\bar{b}_1 = \frac{e_m \bar{c}_1}{V}, \bar{b}_0 = \frac{e_m \bar{c}_0}{V}, \bar{a}_{11} = \bar{a}_{21}, \bar{a}_{10} = \bar{a}_{20} \quad \dots \dots \dots (30)$$

Substituting each coefficient of Eq. (30) into Eq. (14), the state equation becomes the same type as Eq. (20).

4.3 Deriving of control law

The error margin equation is derived by using Eq. (13) and Eq. (20).

$$\begin{aligned} \mathbf{e} &= \mathbf{y} - \mathbf{y}_m = \mathbf{C}\mathbf{x} - \mathbf{C}_m\mathbf{x}_m = \mathbf{x} - \mathbf{C}_m\mathbf{x}_m \\ \dot{\mathbf{e}} &= \dot{\mathbf{y}} - \dot{\mathbf{y}}_m = \mathbf{C}\dot{\mathbf{x}} - \mathbf{C}_m\dot{\mathbf{x}}_m = \mathbf{x} - \mathbf{C}_m(\mathbf{A}_m\mathbf{x}_m + \mathbf{b}_m\theta) \\ &= \mathbf{A}_x + \mathbf{B}\mathbf{u} - \mathbf{C}_m(\mathbf{A}_m\mathbf{x}_m + \mathbf{b}_m\theta) \\ &= \mathbf{A}(\mathbf{x} - \mathbf{C}_m\mathbf{x}_m) + \mathbf{A}\mathbf{C}_m\mathbf{x}_m + \mathbf{B}\mathbf{u} - \mathbf{C}_m\mathbf{A}_m\mathbf{x}_m - \mathbf{C}_m\mathbf{b}_m\theta \\ &= \mathbf{A}\mathbf{e} + (\mathbf{A}\mathbf{C}_m - \mathbf{C}_m\mathbf{A}_m)\mathbf{x}_m + \mathbf{B}\mathbf{u} - \mathbf{C}_m\mathbf{b}_m\theta \end{aligned}$$

Setting more than the right second term as $\mathbf{B}\mathbf{u}_b$, the following equation is obtained.

$$\dot{\mathbf{e}} = \mathbf{A}\mathbf{e} + \mathbf{B}\mathbf{u}_b \quad \dots \dots \dots (31)$$

where

$$\mathbf{B}\mathbf{u}_b = (\mathbf{A}\mathbf{C}_m - \mathbf{C}_m\mathbf{A}_m)\mathbf{x}_m + \mathbf{B}\mathbf{u} - \mathbf{C}_m\mathbf{b}_m\theta \quad \dots \dots \dots (32)$$

Next, it is defined that \mathbf{u} is sum with feed forward term \mathbf{u}_f and feed back term \mathbf{u}_b .

$$\mathbf{u} = \mathbf{u}_f + \mathbf{u}_b \quad \dots \dots \dots (33)$$

Eq. (33) is substituted for Eq. (32).

$$\begin{aligned} \mathbf{B}\mathbf{u}_b &= (\mathbf{A}\mathbf{C}_m - \mathbf{C}_m\mathbf{A}_m)\mathbf{x}_m + \mathbf{B}(\mathbf{u}_f + \mathbf{u}_b) - \mathbf{C}_m\mathbf{b}_m\theta \\ \mathbf{B}\mathbf{u}_f &= -(\mathbf{A}\mathbf{C}_m - \mathbf{C}_m\mathbf{A}_m)\mathbf{x}_m + \mathbf{C}_m\mathbf{b}_m\theta \end{aligned}$$

Therefore, the feed forward control input is given by the next equation.

$$\mathbf{u}_f = -\mathbf{B}^{-1}\{(\mathbf{A}\mathbf{C}_m - \mathbf{C}_m\mathbf{A}_m)\mathbf{x}_m - \mathbf{C}_m\mathbf{b}_m\theta\} \quad \dots \dots \dots (34)$$

In addition, Laplace transform is done to both sides of first equation of Eq. (20).

$$\begin{aligned} s\mathbf{x}_m &= \mathbf{A}_m\mathbf{x}_m + \mathbf{b}_m\theta \\ (s\mathbf{I} - \mathbf{A}_m)\mathbf{x}_m &= \mathbf{b}_m\theta \\ \mathbf{x}_m &= (s\mathbf{I} - \mathbf{A}_m)^{-1}\mathbf{b}_m\theta = P_m\theta \quad \dots \dots \dots (35) \end{aligned}$$

where, P_m is a transfer function of the state variable output to the input of steering wheel angle.

Substituting Eq.(35) into Eq.(34), next Eq.(36) is obtained.

$$\begin{aligned} \mathbf{u}_f &= -\mathbf{B}^{-1}\{(\mathbf{A}\mathbf{C}_m - \mathbf{C}_m\mathbf{A}_m)(s\mathbf{I} - \mathbf{A}_m)^{-1} - \mathbf{C}_m\}\mathbf{b}_m\theta \\ &= G_{ff}(s)\theta \quad \dots \dots \dots (36) \end{aligned}$$

In a word, we can understand that \mathbf{u}_f is a feed forward control input by the steering wheel angle. Moreover, the transfer function is shown by $G_{ff}(s)$.

Facilitating to calculate when we use the control design software Matlab, we obtain \mathbf{x}_m directly from Eq. (35) beforehand. The next equation is derived by using the first equation of Eq. (20).

$$\mathbf{x}_{m\beta} = (s\mathbf{I} - \mathbf{A}_{m\beta})^{-1}\mathbf{b}_{m\beta}\theta$$

where

$$s\mathbf{I} - \mathbf{A}_{m\beta} = \begin{bmatrix} s & -1 \\ \bar{a}_{10} & s + \bar{a}_{11} \end{bmatrix} = \mathbf{A}_b$$

$$(s\mathbf{I} - \mathbf{A}_{m\beta})^{-1} = \frac{1}{|\mathbf{A}_b|}\tilde{\mathbf{A}}_b$$

$$|\mathbf{A}_b| = s^2 + \bar{a}_{11}s + \bar{a}_{10}$$

$$\tilde{\mathbf{A}}_b = \begin{bmatrix} s + \bar{a}_{11} & 1 \\ -\bar{a}_{11} & s \end{bmatrix}: \text{adjugate matrix}$$

Therefore, the next equation is obtained.

$$\mathbf{x}_{m\beta} = \begin{bmatrix} x_{m1} \\ x_{m2} \end{bmatrix} = \frac{1}{s^2 + \bar{a}_{11}s + \bar{a}_{10}} \cdot \begin{bmatrix} 1 \\ s \end{bmatrix} \theta \quad \dots \quad (37)$$

In the same way, the next Eq. (38) is obtained by using the second equation of Eq.(20).

$$\mathbf{x}_{mr} = (s\mathbf{I} - \mathbf{A}_{mr})^{-1} \mathbf{b}_{mr} \theta$$

$$\mathbf{x}_{mr} = \begin{bmatrix} x_{m3} \\ x_{m4} \end{bmatrix} = \frac{1}{s^2 + \bar{a}_{21}s + \bar{a}_{20}} \cdot \begin{bmatrix} 1 \\ s \end{bmatrix} \theta \quad \dots \quad (38)$$

When Eq. (37) and Eq. (38) are brought together in one, the next equation is obtained.

$$\mathbf{x}_m = \begin{bmatrix} \mathbf{x}_{m\beta} \\ \mathbf{x}_{mr} \end{bmatrix} = \begin{bmatrix} 1/(s^2 + \bar{a}_{11}s + \bar{a}_{10}) \\ s/(s^2 + \bar{a}_{11}s + \bar{a}_{10}) \\ 1/(s^2 + \bar{a}_{21}s + \bar{a}_{20}) \\ s/(s^2 + \bar{a}_{21}s + \bar{a}_{20}) \end{bmatrix} \theta \quad \dots \quad (39)$$

Next, we decide the feedback control input element \mathbf{u}_b .

In this report, we handle Eq. (31) as the optimum regulator problem, and derive \mathbf{u}_b that can minimize the performance function J .

$$J = \int_0^\infty (\mathbf{e}^T \mathbf{Q} \mathbf{e} + \mathbf{u}_b^T \mathbf{R} \mathbf{u}_b) dt \quad \dots \quad (40)$$

Here, \mathbf{Q} and \mathbf{R} are the arbitrary weight putting constant matrix.

\mathbf{u}_b is decided by next Eq. (41).

$$\mathbf{u}_b = -\mathbf{R}^{-1} \mathbf{B}^T \mathbf{P} \mathbf{e} = G_{fb}(s) \mathbf{e} \quad \dots \quad (41)$$

\mathbf{u}_b is the feedback control input based on the error margin \mathbf{e} between actual state variables and virtual state variables by the reference model. The transfer function from \mathbf{e} to \mathbf{u}_b is shown by $G_{fb}(s)$.

By the way, \mathbf{P} in Eq. (41) is only solution of the following Riccati equation known well and is the positive-definite symmetric matrix.

$$\mathbf{P} \mathbf{A} - \mathbf{P} \mathbf{B} \mathbf{R}^{-1} \mathbf{B}^T \mathbf{P} + \mathbf{Q} + \mathbf{A}^T \mathbf{P} = \mathbf{0} \quad \dots \quad (42)$$

Substituting \mathbf{P} obtained by solving Eq. (42) into Eq. (41), \mathbf{u}_b is obtained.

And, substituting Eq. (36) and Eq. (41) into Eq. (33), \mathbf{u} is decided as follows.

$$\mathbf{u} = -\mathbf{B}^{-1} \{ (\mathbf{A} \mathbf{C}_m - \mathbf{C}_m \mathbf{A}_m)(s\mathbf{I} - \mathbf{A}_m)^{-1} - \mathbf{C}_m \} \mathbf{b}_m \theta - \mathbf{R}^{-1} \mathbf{B}^T \mathbf{P} \mathbf{e}$$

$$= G_{ff}(s) \theta + G_{fb}(s) \mathbf{e} \quad \dots \quad (43)$$

The block diagram showing the relations between Eqs. (13), (20) and (43) is illustrated in Figure 5.

5 . Calculation and consideration

We take up the case of setting the target transfer function of yaw rate to the first/second form and of making the yaw center a prescribed position ($e = 0$) (the case of ③ in clause 4.2) as a calculation example. Each coefficient of the reference model uses the target value shown in clause 3.4. These weighting matrices assume that they are constant to the change in vehicle velocity. We compare with the front-rear wheel active-steering and 2WS in calculations.

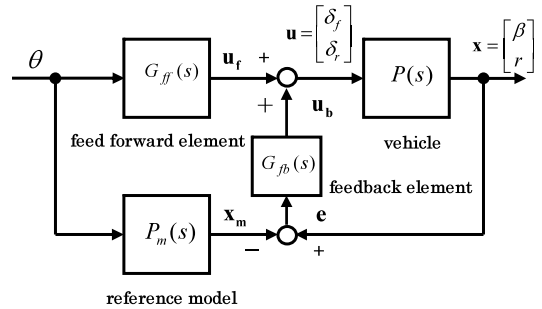


Fig.5 Block diagram of four-wheel active steer control system

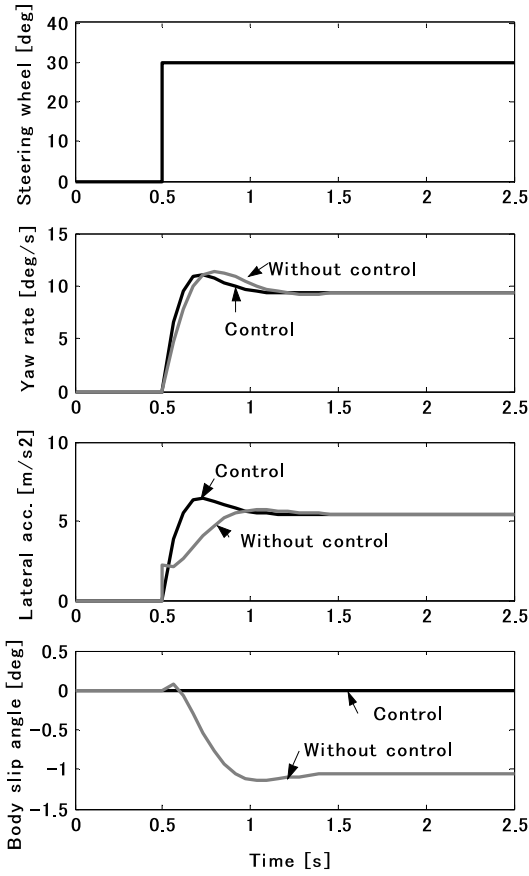


Fig.6 Step response characteristics

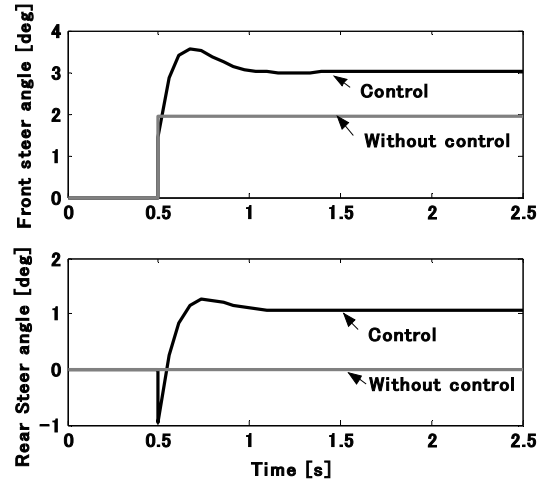


Fig.7 Step response characteristics of front and rear tire steer angles

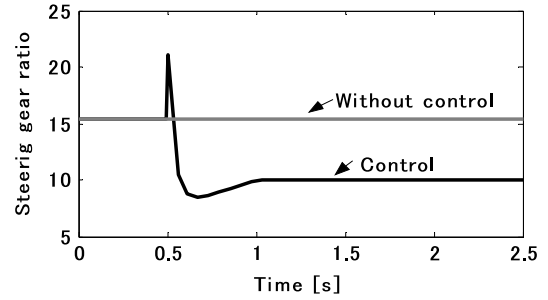


Fig.8 Comparison of changes in equivalent steering gear ratio of front wheel

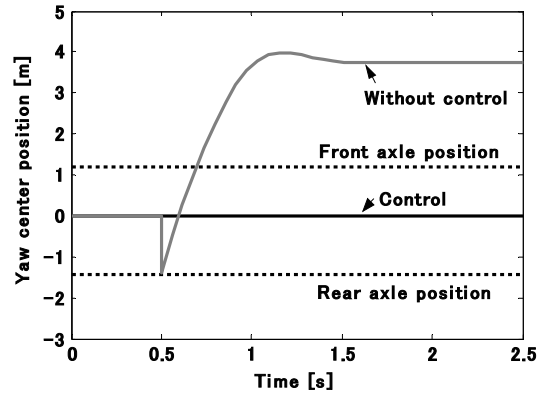


Fig.9 Comparison of changes in yaw center position

The step response and the frequency response to the steering wheel angle input are examined as an open-loop control system. The vehicle velocity at this time assumes 120[km/s].

Moreover, to investigate the control performance of the driver-vehicle system as a closed-loop control system considering the driver's control action characteristics, we carry out the computational simulation us-

ing the Runge-Kutta method in which the driver was asked to execute lane changes during quick braking.

5.1 Step response

Figure 6 shows the step response characteristics for the steering wheel angle 30[deg]. The control vehicle perform that yaw rate follows a target characteristic securing fast rise time and moderate transient overshoot compared with 2WS. The lateral acceleration also increases quickly and is greatly generated immediately after the step operating input of steering wheel. The body slip angle is zero according to the control objective at all times, and it greatly improves cornering performance compared to 2 WS.

Figure 7 shows the changes of front and rear wheel steer angles. The maximum real steer angle of front wheel is about 3.5[deg] at transient overshoot. Moreover, the steer angle of rear wheel reverses from the opposite phase to the same phase, and the maximum real steer angle is about -1 and 1[deg] in these two states respectively.

Figure 8 shows the changes in equivalent steering gear ratio of front wheel.

Figure 9 shows the changes in yaw center position. Here, because yaw center doesn't exist when going straight, we assumed it to be the center of gravity in the calculation expediently. The yaw center of 2 WS greatly exceeds the front wheel position from the rear wheel position and moves forward of the vehicle greatly. On the other hand, the yaw center of control vehicle is always fixed to the center of gravity according to the target.

5.2 Frequency response

Figure 10 shows the frequency response characteristics of yaw rate and lateral acceleration to steering wheel angle. The unit of the gain displays [1/s] and [m/s²/rad] by [dB] respectively. Yaw rate characteristic of the control vehicle corresponds to the reference model. In addition, the lateral acceleration α_y is transformed to the following expression by using Eq. (28) and $e=0$.

$$\alpha_y = V(s\beta + r) = (se + V)r = Vr \quad (44)$$

Equation (44) shows that the lateral acceleration gain is

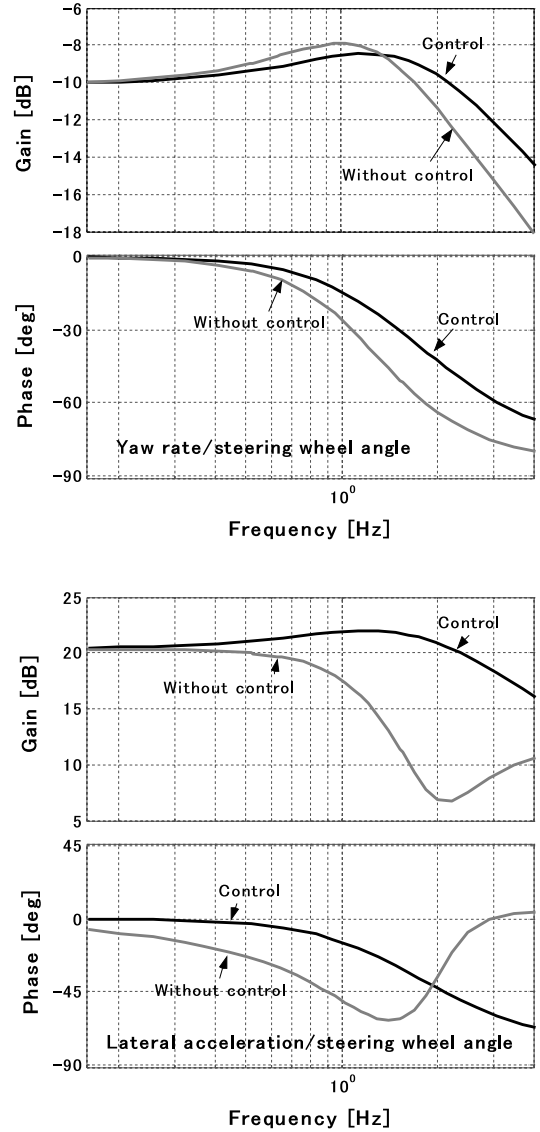


Fig.10 Frequency response characteristics

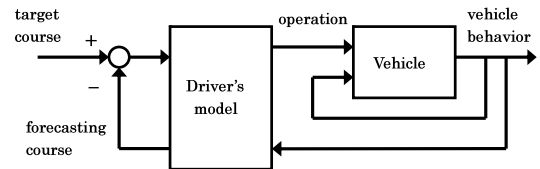


Fig.11 Block diagram of closed-loop system

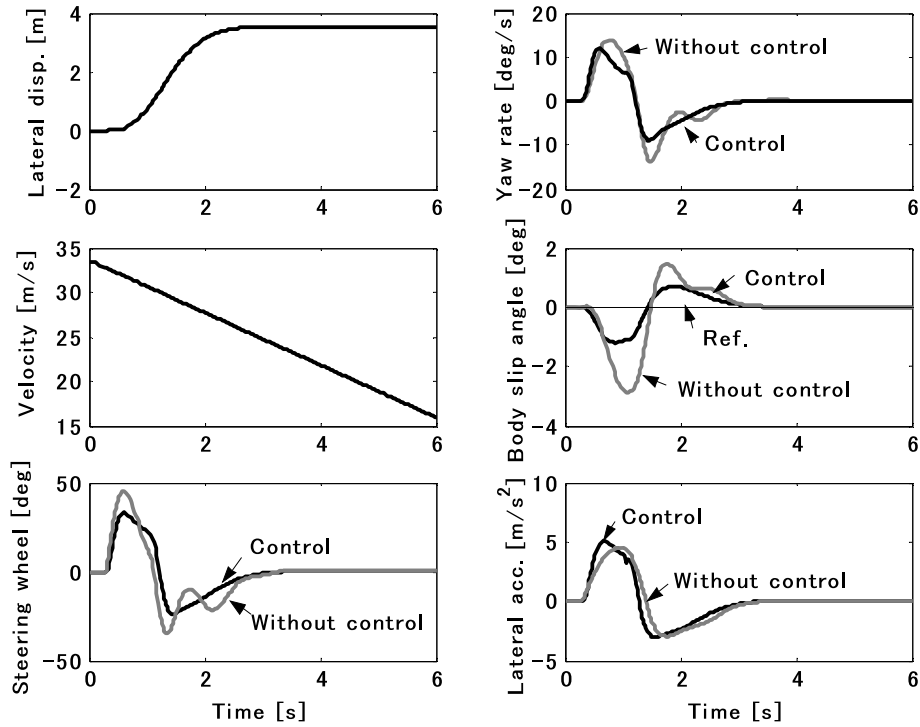


Fig.12 Lane change with deceleration

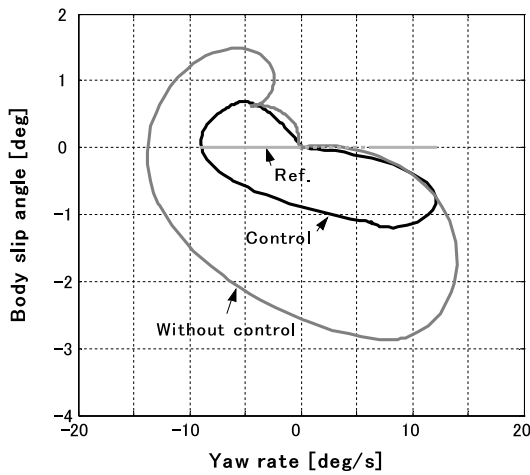


Fig.13 Relationship between yaw rate and body slip angle

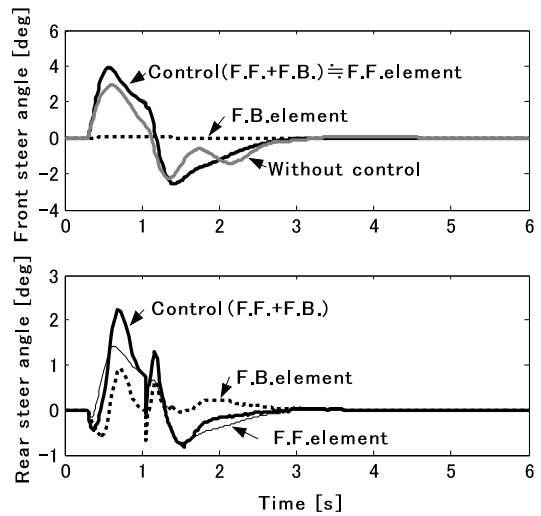


Fig.14 Comparison of changes in front and rear steer angles during lane change with deceleration

a parallel movement of the graph of yaw rate in the vertical direction, and its phase lag is the same as the phase lag of yaw rate. Therefore, as for the control vehicle, both decreases in the gain of the yaw rate and the lateral acceleration are small, and the phase lags are also small in the range of steering input frequency 1 [Hz] or more. Especially, when the difference of phase lag of yaw rate and lateral acceleration is zero.

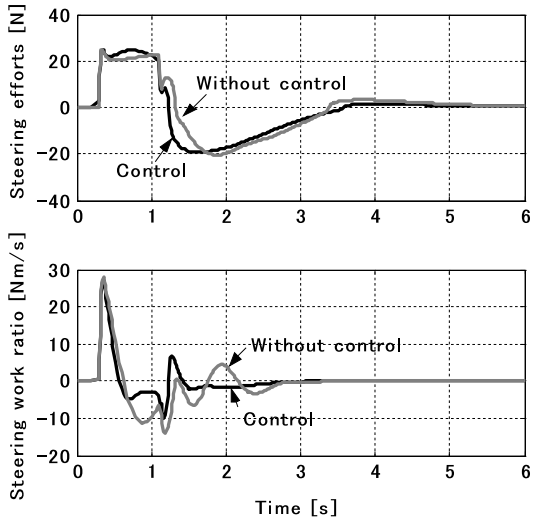


Fig.15 Comparison of changes in work and power of steering wheel control

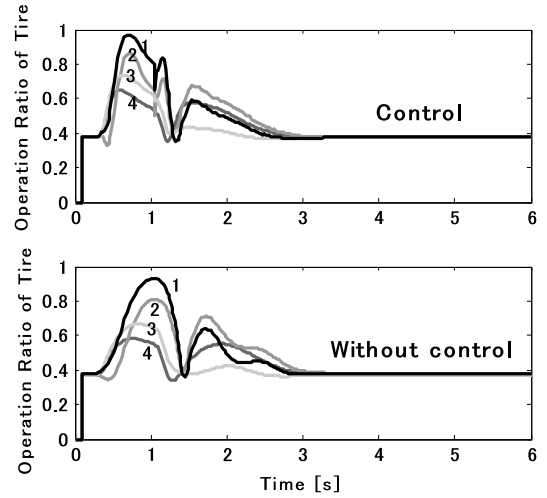


Fig.16 Comparison of changes in availability of tire forces

5.3 Lane change maneuver

The block diagram of driver-vehicle system in computer simulation is illustrated in Figure 11. This running situation of the vehicle simulates maneuverability and stability during emergency obstacle avoidance. The lane changing with deceleration by braking 0.3 [G] at an initial velocity of 120 [km/h] is simulated. We apply the first-order prediction model using the feedback of lateral error from a desired course to the driver's fixation point as driver's control action model. Steering wheel angle as the output of this model is input to θ in Eq. (43). The driving lane where the test vehicle runs requires a setting where the lateral motion of 3.5 [m] between the slant distances of 25 [m]. Each tire of the vehicle considers the load transfer between front wheel and rear wheel, and between right wheel and left wheel generated by the cornering motion with braking. The mathematical modeling that has nonlinear cornering characteristics for sideslip angle and vertical load of tire is used for the tire characteristic. The test road is smooth, and the maximum coefficient of static friction and the coefficient of dynamic friction are assumed to be 1.0 and 0.8 respectively.

Figure 12 shows the calculated result of vehicular swept path of the center of gravity while lane changing, vehicle velocity, steering wheel angle and vehicle's dynamic characteristics. Lissajous curves in Fig.13 show the relation between yaw rate and body sideslip angle. As for the control vehicle, both yaw rate and lateral acceleration are faster than those of 2WS increasing immediately after beginning of steering input. In addition, body sideslip angle and yaw rate are controlled, there is no useless movement in the control vehicle, and the amount of maneuvering to the steering wheel can be also be reduced. Therefore, the driver can maneuver the steering wheel in a stable way when the steering wheel counterreacts. In the computer simulation, we set a severe driving condition to generate comparatively large longitudinal acceleration and lateral acceleration at high speed, and the calculation results show that the control vehicle has good response and stable behavior despite performing urgent maneuvers for accident evasion.

Figure 14 shows the comparison of changes in front and rear steer angles. In this calculation, the total real steer angles are separate to the feed forward element and the feedback element. The total real steer angle of front wheel is more than that of 2WS, and most is the feed forward element. On the other hand, the pro-

portion of the feedback element is large in the rear wheel. Here, though there is a disorder in the shape of the waves of rear wheel steer angle after about one second, we think the cause could be the following: The driver model's maneuvers became discontinuous because the target lane is discontinuous, too and, the calculation of the feedback element became temporarily unstable for this. However, this didn't influence the state variables of the vehicle motion.

To examine the driver's physical load the workload and the power at the steering wheel maneuvers are calculated by using an easy two-degree-of-freedom calculation model of the steering device. Figure 15 shows the calculation results. Two physical quantities of the control vehicle are smaller than those of 2WS. And, as for the power, the difference between the control vehicle and 2WS is large.

Next, to examine the operating situation of longitudinal and lateral forces to the maximum frictional force of the tires, each tire availability of the four-wheel is calculated. Figure 16 shows the change of tire availability to the time in each wheel. The number of 1 ~ 4 on the graph sequentially represents a right-front wheel, a right-rear wheel, a left-front wheel and a left-rear wheel in this figure. It is confirmed that the control vehicle can quickly start up the tire force, and use the tire force effectively.

6 . Conclusions

We clarified the following results for the active steer control system of front and rear wheels.

- (1) We showed the method of setting concrete target vehicle motion characteristics to drive more easily, and obtained the steer control rule for controlling two vehicle motion state variables of yaw rate, and body slip angle or yaw center position at the same time based on the requested target ones.
- (2) We obtained the control rule that combines the feed forward control of steering wheel angle and the feedback control of vehicle state variables, which has the reference model of setting the yaw rate characteristic to a target transfer function of the first/second form and the yaw center position to a center of gravity of the vehicle.
- (3) Computer simulation clarified that the vehicle applied to the control rule of above-mentioned (2) can achieve a good control effect, even in the range where such the tire cornering characteristics as the lane change maneuver with a deceleration are nonlinear.

Appendix

Coefficients of Eq. (6)

$$K = \frac{m}{2l^2} \left(\frac{b}{K_f} - \frac{a}{K_r} \right) \quad \cdot \cdot \cdot \quad \text{Stability factor}$$

$$G_{\beta 1} = \frac{1 - \frac{m}{l} \cdot \frac{aV^2}{2bK_r}}{1 + KV^2} \cdot \frac{a}{l} \quad \tau_{\beta 1} = \frac{I_z V}{2lbK_r - maV^2} \quad G_{\beta 2} = \frac{1 - \frac{m}{l} \cdot \frac{bV^2}{2bK_f}}{1 + KV^2} \cdot \frac{a}{l} \quad \tau_{\beta 2} = \frac{I_z V}{2laK_f - mbV^2}$$

$$G_{r1} = \frac{1}{1 + KV^2} \cdot \frac{V}{l} \quad \tau_{r1} = \frac{maV}{2lK_r} \quad G_{r2} = \frac{-1}{1 + KV^2} \cdot \frac{V}{l} \quad \tau_{r2} = \frac{mbV}{2lK_f}$$

$$\omega_n = \frac{2l}{V} \sqrt{\frac{K_f K_r}{mI_z} (1 + KV^2)} \quad \zeta = \frac{(ma^2 + I_z)K_f + (mb^2 + I_z)K_r}{2l\sqrt{mI_z K_f K_r} (1 + KV^2)}$$

References

- (1) Mori,K., Eguchi,T., Kaneko,S., Kawagoe,K. and Irie,N., Improvement in Maneuverability and Stability through Transient Steer Control of Four-wheel-steering in Consideration of Suspension Characteristics,

- Transactions of Society of Automotive Engineers of Japan*, No.45 (1990), pp.31-36.
- (2) Mori,K., Response Analysis for Four-Wheel-Steering Vehicle to Steering Inputs under Cornering Motion, *Transactions of the Japan Society of Mechanical Engineers, Series C*, Vol.59, No.560 (1993), pp.112-117.
 - (3) Inoue,H. and Sugasawa,F., Improvement of Vehicle Dynamics through 4WS with State Feedback Control, *Transactions of Nissan Technical Review*, (1993), pp.13-19.
 - (4) Sugasawa,F., Irie,N., Kuroki,J., Fukunaga,Y. and Nakamura,K., Improvements in Vehicle Control and Stability through Front-and Rear-Wheel Steering Control, *Transactions of Society of Automotive Engineers of Japan*, No.38 (1988), pp.62-70.
 - (5) Furukawa,Y., Takei,A., Kobayashi,M. and Kawai,T., Effects of Active Steering Control on Closed-Loop Control Performance of Driver-Vehicle System, *Proceedings of JSAE Annual Congress (Autumn)*, No.902, 902180, (1990-10), pp.1. 325-1. 328.
 - (6) Mori,K., Improvement in Maneuverability and Stability of Vehicle through Front/rear Active Steering Control with Steer-by-wire, *Bulletin of Kurume Institute of technology*, No.30 (2007), pp.37-46.
 - (7) Nagai,M., Yamanaka,S., Saito,Y. and Hirano,Y., Study Integrated Control of Active Rear Wheel Steering and Braking/Traction Forces, *Proceedings of JSAE Annual Congress (Spring)*, No.972, 9732216, (1997-5), pp.29-32.
 - (8) Katayama,T., Yasuno,Y., Oida,T., Sao,M., Imamura,M., Seki,N. and Sato,Y., Development of 4Wheel Active Steer, *Proceedings of JSAE Annual Congress (Spring)*, No.11-07, 20075281, (2007-5), pp.7-12.
 - (9) Noguchi,H., Kaneko,S., Uehara,K., Ogino,K. and Asai,T., Application of Measurement Technologies and CAE to the Vehicle Dynamics of the New SKYLINE, *Nissan Technical Review*, No.60 (2007-3), pp.20-25.
 - (10) Mori,K. and Kajiyama,K., Influence that Steer Characteristics of Suspension exerts on Driver's Driving Behavior, *Bulletin of Kurume Institute of technology*, No.30 (2007), pp.29-36.
 - (11) Irie,N. and Shibahata,Y., Influence of Rear Suspension Characteristic on Maneuverability and Stability of Automobile, *Journal of Society of Automotive Engineers of Japan*, Vol.39, No.3 (1985), pp.275-285.
 - (12) Masato Abe, *Dynamics and Control of Automobile (The second edition)* (in Japanese), ISBN 4-381-08822-0, (2003), pp.234-236, SANKAIDO.
 - (13) Eguchi,T., Sakita,Y., Kawagoe,K., Kaneko,S., Mori,K. and Matsumoto,T., Development of "Super Hicas" a New Rear Wheel Steering System with Phasereversal Control, *SAE Technical Paper*, 891978, (1989-9), pp.1-10.
 - (14) Mori,K., Eguchi,T., Kaneko,S., Kawagoe,K. and Irie,N., Improvement in Vehicle Control and Stability through Optimizing the Transient Steer Characteristics of 4 Wheel Steering---SUPER HICAS, *Proceedings of JSAE Annual Congress (Spring)*, No.891, 891068, (1989-5), pp.279-282.
 - (15) Iguchi,M., Cooperative Steering Control between Front and Rear Wheels in 4-wheel-steering Cars, *Transactions of Society of Automotive Engineers of Japan*, No.35 (1987), pp.120-125.
 - (16) Nakamoto,M. and Kaneshina,N., Effect of Four-wheel Steering System on Vehicle Yawing Motion, *Journal of Society of Automotive Engineers of Japan*, Vol.42, No.3 (1988), pp.289-296.